

## Formation and evolution of bars in disc galaxies

E. Athanassoula

*Observatoire de Marseille, 2 Place Le Verrier, 13248 Marseille cedex 04,  
France*

**Abstract.** I follow a bar from its formation, via its evolution, to its destruction and, perhaps, regeneration. I discuss the main features at each stage and particularly the role of the halo. Bars can form even in sub-maximum discs. In fact, such bars can be stronger than bars which have grown in maximum discs. This is due to the response of the halo and, in particular, to the exchange of energy and angular momentum between the disc particles constituting the bar and the halo particles at resonance with it. The bar slowdown depends on the initial central concentration of the halo and the initial value of the disc  $Q$ . Contrary to the halo mass distribution, the disc changes its radial density profile considerably during the evolution. Applying the Sackett criterion, I thus find that discs become maximum in many simulations in which they have started off as sub-maximum. I briefly discuss the evolution if a gaseous component is present, as well as the destruction and regeneration of bars.

### 1. Introduction

Bars can form spontaneously in galactic discs (e.g. Miller, Prendergast & Quirk 1970, Hohl 1971). They then evolve over a large number of rotations, changing their length, strength, shape and angular frequency. During this period they can drive spiral or ring formation, push gas to the center-most parts of the galaxy and thus trigger starbursts and activity in the nucleus, and interact with the outer disc, bulge and/or halo by exchanging energy and angular momentum with them. I will discuss a few of these processes, relying – due to the strongly nonlinear nature of bars – mainly on results of  $N$ -body simulations.

### 2. Simulations

The results presented in sections 3 to 6 come from a preliminary analysis of well over 100 simulations run on our GRAPE-5 systems (Kawai et al. 2000). Six of these have been discussed by Athanassoula & Misiriotis (2002, hereafter AM) and Athanassoula (2002, hereafter A02), where more information on the numerical techniques can be found. Initially the disc is always exponential radially, and follows an  $sech^2$  law with scalelength  $z_0$  in the vertical direction. Its initial  $Q$  value (hereafter  $Q_{init}$ ) does not vary with radius. The disc mass ( $M_d$ ) and initial scalelength ( $h$ ) will be used as units of mass and length in the simulations. The halo is initially isotropic and non-rotating, and follows the density law

$$\rho_h(r) = \frac{M_h}{2\pi^{3/2}} \frac{\alpha}{r_c} \frac{\exp(-r^2/r_c^2)}{r^2 + \gamma^2}, \quad (1)$$

where  $\alpha$  is a normalisation constant,  $M_h$  is the mass of the halo and  $\gamma$  and  $r_c$  are scalelengths. This functional form contains three free parameters and thus allows a large flexibility. For relatively large values of  $\gamma$  the halo profile resembles those used by observers in rotation curve decompositions, and is thus observationally motivated. On the contrary, for sufficiently small values of  $\gamma$  the halo rotation curve rises very steeply, thus mimicking a cusp in the halo distribution. Indeed, the core can be chosen sufficiently small to be hidden by the softening length. In all the simulations discussed here, except for the ones mentioned in the end of section 6,  $M_h = 5$  and  $r_c = 10$ .

The total number of particles per simulation varies between 1 and 1.5 million. I adopted a softening of 0.0625 and a time-step of 0.015625. I assessed the numerical robustness of my results by trying in a few cases double the number of particles, different values of the softening and time step, as well as direct summation (with half the number of particles) and a non-GRAPE tree code. Various calibrations are possible. AM proposed to set the unit of length equal to 3.5 kpc and the unit of mass to  $5 \times 10^{10} M_\odot$ . In this case  $t = 500$  corresponds to 7 Gyrs. Alternatively, one could use a considerably smaller value in kpc for the disc scalelength, arguing that this is the *initial* disc scalelength and that this length will increase with time. Thus opting for a 2 kpc scalelength would set  $t = 500$  to roughly 3 Gyrs. Time, in particular, may be difficult to calibrate, since numerical parameters, like the softening and the number of particles, can influence the rate at which the bar grows in the initial stages of the simulation. Thus the clock may tick differently, at least for certain parts of the evolution, in simulations than in real galaxies. For these reasons, here we will stay with computer units, allowing the reader the freedom to convert them to astronomical units according to his/her preferences and needs.

The two parameters in the initial conditions influencing most the evolution are the central concentration of the halo and  $Q_{init}$ . The former is given by the parameter  $\gamma$ , which can be thought of as the core radius of the halo.

### 3. The effect of halo central concentration

Figure 1<sup>1</sup> compares three simulations. The one illustrated in the left column of panels has  $\gamma = 5$  and its inner parts are disc dominated from the onset (upper left panel). I will hereafter refer to it as model MD, for massive disc. The middle and right panels refer to simulations with  $\gamma = 0.5$ . Here the halo is much more centrally concentrated and contributes to the total circular velocity curve somewhat more than the disc up to roughly two disc scalelengths, and considerably more at larger radii (middle and left upper panels). I will refer to these two simulations as MH, for massive halo, and RH, for rigid halo, respectively. Indeed in simulation MH, as in MD, the halo is live, i.e. composed of particles, while

---

<sup>1</sup>In the third row of panels, giving the face-on view, I used density values for the isocontours such as to show the structure in the bar region, but leaving out the disc region at larger radii.

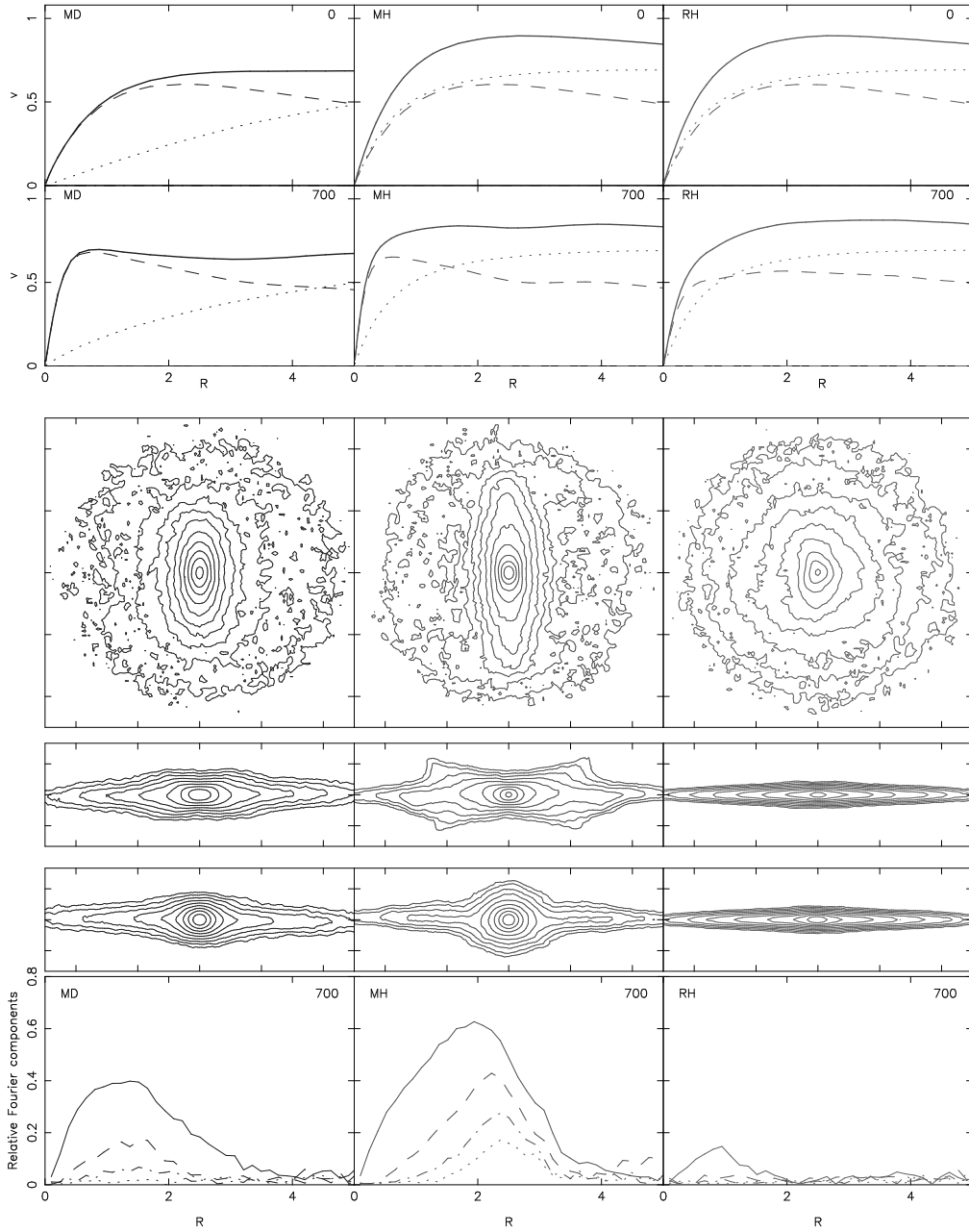


Figure 1. The two upper rows of panels give the circular velocity curves (solid lines) and the contribution of the disc (dashed) and the halo (dotted). The first row is for  $t = 0$ , the second for  $t = 700$ . The next three rows give the isodensities of the disc component when seen face-on (third row) and edge-on, again for  $t = 700$ . In the fourth row the bar is seen side-on and in the fifth end-on. The size of the square box for the third row of panels is  $10h$ . The last row shows the relative Fourier components as a function of radius ( $AM$ ). The  $m = 2, 4, 6$  and  $8$  components are given by solid, dashed, dot-dashed and dotted lines.

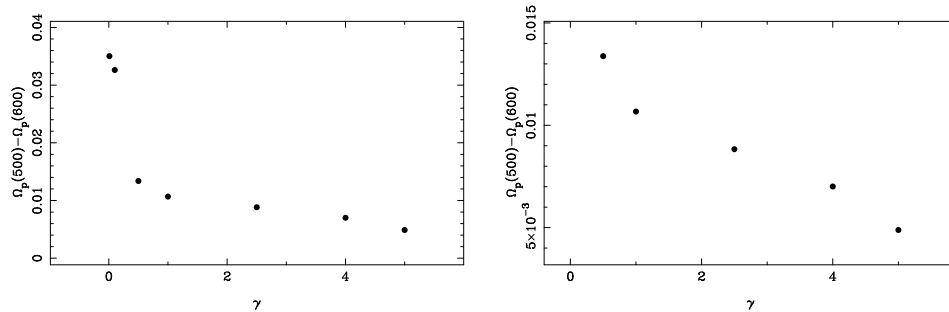


Figure 2. Left panel : Slowdown of the bar pattern speed between times 500 and 600 as a function of the halo central concentration. For these simulations initially  $Q_{init} = 1.2$  and  $z_0 = 0.2$ . Right panel : Blow-up of the lower part of the left panel, showing that the trend with central concentration is clear even for higher values of  $\gamma$ .

in simulation RH it is rigid, i.e. is described by a force and potential imposed on the disc particles. All three simulations start off with  $Q_{init} = 1.2$ .

The differences between the results of simulations MD and MH are very important. The bar in model MH is longer and stronger than that in model MD. Its isodensities are more rectangular-like and, seen edge-on with the bar seen side-on, it displays an ‘X’ shape, while for the same orientation MD shows a boxy structure. Both shapes have been observed in edge-on galaxies. Seen end-on, MD again shows a boxy structure, while MH shows a spheroidal feature of considerable vertical extent. If such a feature was observed in an edge-on galaxy, it would be erroneously classified as a sizeable bulge component. Thus a number of observed bulges could in fact be bars seen end-on. A final, very important difference can be seen by comparing the relative Fourier components of the two models (AM). Model MH has a considerably larger  $m = 2$  component. More important, it has also considerable  $m = 4, 6$  and  $8$  components, very much in agreement with what is observed in early type barred spirals (e.g. Ohta 1996). On the contrary the Fourier components of model MD are more reminiscent of those of late type galaxies. All these differences are surprising and most of them are contrary to previous wisdom, since *the stronger bar is found in the more halo dominated galaxy*.

#### 4. Evolution of some basic quantities

The evolution does not stop after the initial phases of bar formation. I will here describe the evolution of some basic properties, namely the strength and pattern speed of the bar and the angular momentum and mass distribution in the disc and halo components.

##### 4.1. Pattern speed

Due to the interaction with the halo and the outer disc, the bar gradually slows down (see e.g. Tremaine & Weinberg 1984, Weinberg 1985, Combes et al. 1990, Little & Carlberg 1991, Hernquist & Weinberg 1992, Athanassoula 1996, De-

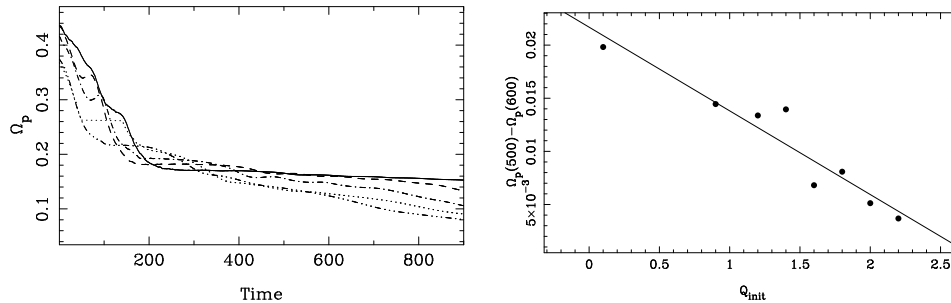


Figure 3. Left panel : Bar pattern speed as a function of time, for  $Q_{init} = 1.4$  (dot-dot-dot-dashed), 1.6 (dotted), 1.8 (dot-dashed), 2 (dashed) and 2.2 (solid line). Right panel : Slowdown of the bar between times 500 and 600 as a function of  $Q_{init}$ . For these simulations initially  $\gamma = 0.5$  and  $z_0 = 0.2$ .

battista & Sellwood 1998 and 2000). The rate at which this happens depends crucially on the two parameters which mainly influence the evolution, namely  $\gamma$  and  $Q_{init}$ .

Simulations with more centrally concentrated haloes, i.e. of MH-type, show a considerably larger slowdown rate than simulations of MD-type. This is clearly seen in Fig. 2, where I plot the slowdown of the bar between times 500 and 600 as a function of  $\gamma$ . In particular for the smallest values of  $\gamma$ , i.e. 0.01 and 0.1, the slowdown is non negligible. Even for larger values, however, there is a definite trend of decreasing slowdown rate with increasing  $\gamma$  (right panel). This is in good qualitative agreement with the results of Debattista & Sellwood (1998, 2000), who showed that in cases with massive discs there is an acceptable slowdown of the bar, contrary to simulations with massive halo components. A quantitative comparison will be given elsewhere.

The halo mass distribution, however, is not the only parameter influencing the slowdown of the bar. The left panel of Fig. 3 shows the evolution of the pattern speed with time for simulations which have initially identical live haloes and identical mass distributions in the disc component, but different  $Q_{init}$ . It is clear that  $Q_{init}$  influences strongly the bar slowdown, in the sense that bars in initially colder discs show a much stronger slowdown rate than bars in initially hotter discs. This is further explicated in the right panel, where I give the slowdown of the bar between times 500 and 600 as a function of  $Q_{init}$ . The solid line is simply a least squares fit to the data to guide the eye and does not imply that the decrease should be linear.

Thus the slowdown rate is a function of at least two parameters,  $Q_{init}$  and  $\gamma$ , and a particular value of this rate can be achieved not only for a single ( $Q_{init}$ ,  $\gamma$ ) pair, but for a sequence of such pairs. One should, therefore, refrain from using this rate to obtain limits on the values of one of the two parameters, unless the value of the other is relatively well constrained. This should be kept in mind when using arguments based on the bar slowdown in the ongoing debate about whether discs are maximum or sub-maximum, since little is known about  $Q_{init}$ . One could argue that discs were initially very cold, as they were composed mainly of gas, which formed stars with low velocity dispersion. On the other

hand, it could also be argued that discs had initially very inhomogeneous mass distributions with big lumps of matter, whose interactions could heat the initial disc to relatively high temperatures. This, together with the inflow of fresh cool gas from the halo, should then determine  $Q_{init}$ .

If the  $Q_{init}$  is sufficiently large, then the bar will not slow down substantially. Furthermore, if  $Q_{init}$  is intermediate, then the increase in bar length (see §4.2) will compensate for the slowdown, in the sense that  $r_L/a$  (where  $r_L$  the corotation radius and  $a$  the bar length) will remain roughly constant during the evolution. This will be discussed in detail elsewhere (Athanassoula 2002, in preparation). Here let us just note that, since our present knowledge does not allow us to have a clear view of the situation, we should refrain from drawing conclusions, if these are sensitive on the value of  $Q_{init}$ . Finally, the slowdown rate could also be dependent on the resolution of the simulations. However, comparisons of simulations with different resolutions should necessarily involve only simulations with the same or similar  $Q_{init}$ , if these are to give meaningful information on the effect of resolution. This issue will be further discussed elsewhere (Athanassoula 2002, in preparation).

#### 4.2. Bar strength and length

The strength of the bar and its evolution with time also depend crucially on  $\gamma$  and  $Q_{init}$ . The left panel of Fig. 4 compares the evolution of the bar strength for the three simulations already discussed in section 3. The bar strength is here defined as the total  $m = 2$  component of the mass, i.e. integrated over the surface of the disc, divided by the corresponding total  $m = 0$  component. Note that in the initial phases of the evolution the bar grows faster in simulation MD than in MH, in good agreement with the results of the 2D simulations by Athanassoula & Sellwood (1986). At later stages, however, the bar continues growing slowly but steadily in simulation MH, compared to hardly, if at all, in simulation MD. Thus, eventually, the bar in MH becomes considerably stronger than in MD.

The length of the bar in model MD does not show much evolution with time. On the contrary, for model MH it grows considerably with time.

#### 4.3. Angular momentum and mass distribution

During the evolution, the disc gives angular momentum to the halo (see also Debattista & Sellwood 2000) and, as a result, the latter obtains a net rotation in the same sense as the disc. This effect is stronger for MH-type models than for MD-type ones.

As can be seen by comparing the two upper panels of Fig. 1, the disc mass radial profile evolves considerably, becoming much more centrally concentrated. This effect is stronger for initially colder discs. On the other hand the mass distribution in the halo component shows little evolution with time (Fig. 1).

### 5. Maximum versus sub-maximum discs

Observed rotation curves and velocity fields provide useful information on the gravitational forces that act in galactic discs. It is, however, not clear what

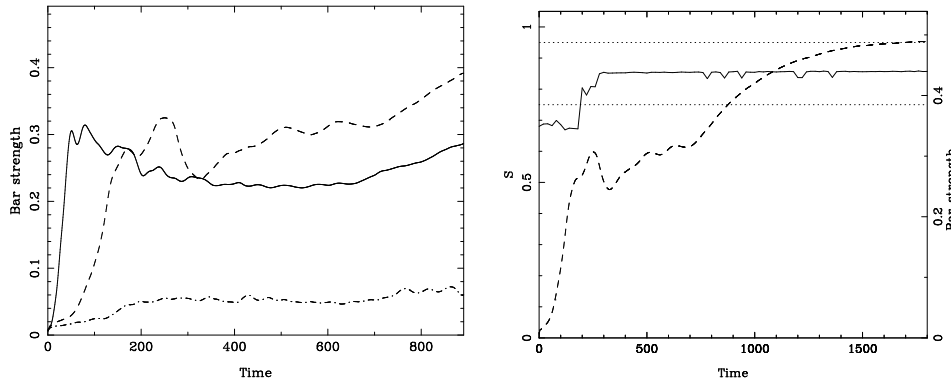


Figure 4. Left panel : Bar strength as a function of time for simulation MD (solid line), MH (dashed) and RH (dot-dashed). Right panel : Evolution of  $S$  as a function of time (solid line) for simulation MH. The two horizontal dotted lines give the limits set by Sackett for a maximum disc. The dashed line gives a measure of the strength of the bar.

fraction of this force is due to the disc and the halo components, respectively. This has been the subject of animated debates, some pieces of evidence arguing that discs are maximum, i.e. that they dominate in the inner regions, and others that their contribution is substantially lower (e.g. Athanassoula, Bosma & Papaioannou 1987; Bosma 1999, 2000 and these proceedings; Bottema 1993; Courteau & Rix 1999; Kranz, Slyz & Rix 2001; Sellwood 1999; Weiner, Sellwood & Williams 2001).

Sackett (1997) and Bosma (2000) give a simple, straightforward criterion, allowing us to distinguish maximum from sub-maximum discs. Consider the ratio  $S = V_{d,max}/V_{tot}$ , where  $V_{d,max}$  is the circular velocity due to the disc component and  $V_{tot}$  is the total circular velocity, both calculated at a radius equal to 2.2 disc scalelengths. According to Sackett (1997) this ratio has to be at least 0.75 for the disc to be considered maximum. Of course in the case of strongly barred galaxies the velocity field is non-axisymmetric and one should consider azimuthally averaged rotation curves, or “circular velocity” curves. Furthermore, in the case of strongly barred galaxies it is not easy to define a disc scalelength, so it is better to calculate  $S$  at the radius at which the disc rotation curve is maximum, which is a well defined radius and is roughly equal to 2.2 disc scalelengths in the case of an axisymmetric exponential disc. After this small adjustment, we can apply the above criterion to our simulations.

As can be seen from Fig. 1, the MD disc starts off as maximum, and its importance increases further with time. On the other hand simulation MH starts as sub-maximum, with a value of  $S$  not far from the value of 0.63 advocated by Bottema (1993). The right panel of Fig. 4 plots the evolution of  $S$  with time and shows clearly that after roughly time 200 the disc becomes maximum, and then stays so, at a roughly constant value of  $S$ . It is interesting to note that the rather abrupt jump of the disc from sub-maximum to maximum happens right after the abrupt increase of the bar strength, i.e. right after bar formation.

In the above example the disc started as sub-maximum and ended as maximum, due to the rearrangement of the disc material. Yet this is not always the case. In cases with strong bulges, small  $\gamma$  and/or large  $Q_{init}$ , the value of  $S$  may not rise sufficiently for the disc to become maximum. The limiting value of  $\gamma$  for which the disc will become maximum after bar formation depends on the values of the remaining parameters of the simulation. Interpolating from a set of simulations with  $Q_{init} = 1.2$ ,  $z_0 = 0.2$  and  $M_h = 5$ , we find the limiting value of  $\gamma$  to be around 0.4. On the other hand, for initially very cold discs, with  $Q_{init} = 0.1$ , the limiting value of  $\gamma$  is much smaller, of the order of 0.13. This last value corresponds to a very fast rising rotation curve, reminiscent of those obtained with a cuspy halo density profile. In fact, since this value of  $\gamma$  is only slightly larger than twice the softening length, a smaller distance would not be well resolved with the present simulations.

We can thus conclude that whether a disc ends as maximum or as sub-maximum depends on the central concentration of the halo and on the initial velocity dispersion in the disc. For highly centrally concentrated but non-cuspy haloes ( $\gamma = 0.5$ ), as those favoured by observers for early type galaxies, an initially sub-maximum disc will become maximum after the bar has formed. This holds for all such initial conditions that I tried, except if  $Q_{init}$  is larger than 1.7. On the other hand, if the haloes are cuspy, then the threshold  $Q_{init}$  is considerably smaller. It should also be noted that the exact position of this threshold may well depend on the initial  $z_0$  and on the halo-to-disc mass ratio – which here has been taken to be equal to 5 – and perhaps also on numerical parameters like the softening. Thus, although the above discussion argues that it is quite likely that discs of strongly barred galaxies are maximum, a considerable amount of work is still necessary in order to produce a rigid criterion.

## 6. The role of the halo

The strongest differences in Fig. 1 are between the middle (model MH) and right (model RH) columns of panels. Indeed, the face-on view of model MH shows a very strong bar and the edge-on one a very strong peanut, or rather an ‘X’-type feature. On the contrary, model RH shows at most a slight oval distortion in the inner parts of the face-on view and not even a boxiness in the edge-on views. Similarly, the rotation curves in the second row of panels reveal that the disc material for model MH has considerably concentrated towards the center, while there is only a very small such effect for RH. Since the two models are initially identical in everything, except that the halo of RH is rigid, while that of MH is live, it must be the halo response that is responsible for the big differences.

In order to understand the halo response we need first to understand its orbital structure. We thus need to calculate, at a given time  $t$ , the principal frequencies of the halo and disc orbits, i.e. the values of the angular frequency  $\Omega$ , the epicyclic frequency  $\kappa$  and the vertical frequency  $\kappa_z$  for each orbit (A02). For this, I calculate the total potential and the bar pattern speed at this time. In this potential, now considered as stationary in a frame of reference rotating with the measured pattern speed, I calculate the orbits of 100 000 disc and 100 000 halo particles and from these their basic frequencies. This reveals that a considerable number of halo stars are in resonance with the bar. Fig. 5 plots the number of



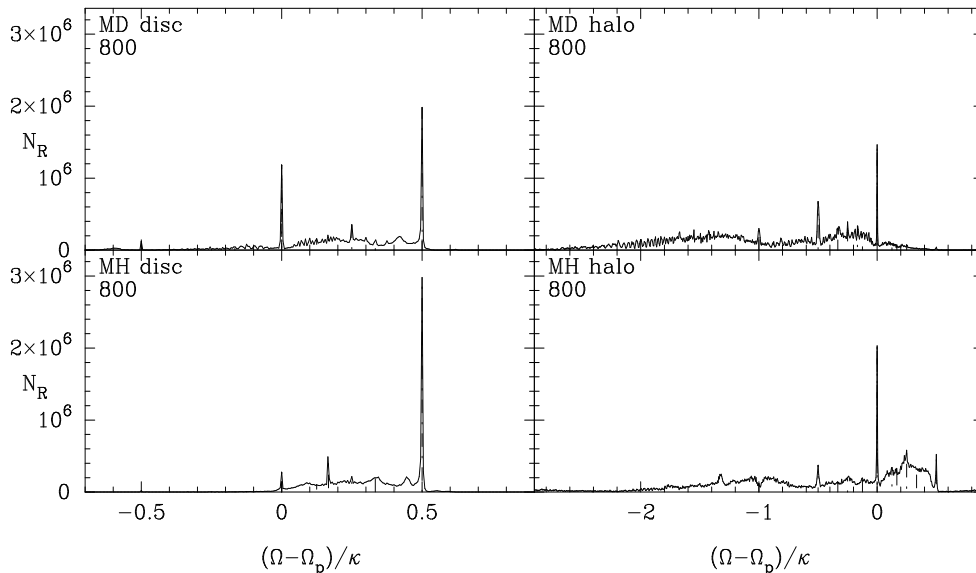


Figure 5. Number density,  $N_R$ , of particles as a function of the frequency ratio  $R_f = (\Omega - \Omega_p)/\kappa$ . The results for the halo component have been rescaled, so as to take into account the different number of particles in the disc and halo components, and thus allow immediate comparisons.

particles (orbits),  $N_R$ , that have a frequency ratio  $R_f = (\Omega - \Omega_p)/\kappa$  within a bin of a given width centered on a value of this ratio, plotted as a function of  $R_f$ . The distribution is far from uniform and shows high peaks at the main resonances, both for the disc and the halo components. Disc particles at inner Lindblad resonance will emit energy and angular momentum (Lynden-Bell & Kalnajs 1972) which can be absorbed either by disc particles at corotation and outer Lindblad resonance, or by halo resonant particles. Since the bar is a negative angular momentum perturbation, the halo, by taking angular momentum from it, helps it grow. Thus haloes, instead of stabilising discs, as was previously thought, can help bars grow. This new instability mechanism (A02) can account for strong bars in cases with strong halo components, and explains why the bar in model MH is stronger than that in model MD.

However, one should not extrapolate this behaviour further to ever stronger halo components and conclude that the stronger the halo the stronger the bar should be. There will obviously be a point where the disc will be comparatively too light to emit all the angular momentum the halo can absorb. For simulations with  $M_h/M_d = 5$  the discs proved to be bar unstable for all the values of  $\gamma$  I tried. This, however, is not always the case for smaller disc-to-halo mass ratios. Thus no bar formed for  $M_h/M_d = 10$  and  $\gamma = 0.5$  at least up to  $t = 900$ , and presumably much longer. This shows that, although bars can grow in sub-maximum discs, they can not grow in galaxies with an arbitrarily small disc contribution.

## 7. Evolution in the presence of gas

The evolution of a barred galaxy containing a considerable amount of gas in the disc can differ substantially from that of a galaxy with no gaseous component.

One of the differences is that the pattern speed may stay constant, or even increase with time, contrarily to what was seen in the purely stellar cases (Friedli & Benz 1993, Heller & Shlosman 1994, Berentzen et al. 1998). Unfortunately not much quantitative information from appropriate  $N$ -body simulations can be found in the literature, and a study of the evolution of the pattern speed for different gas masses and distributions would certainly be most useful. The problem is particularly interesting since in the exchange of energy and angular momentum, discussed in the previous section, a third partner has been added to the stellar disc and the halo components, namely the gas.

As a response to the bar forcing, the gas concentrates in two very narrow and elongated regions near the leading edges of the bar, which are in fact the loci of shocks. Depending on the bar parameters, and in particular its strength, they are either straight, or curved with their concave side towards the bar major axis (Athanassoula 1992). As a result of these shocks, the gas flows inwards and accumulates in an area near the center. The size of this central area is of the order of a kpc, and is determined by the extent of the largest orbits of the  $x_2$  family.

In order to come yet further inwards, to the nucleus of the galaxy, the gas has to shed a yet larger fraction of its angular momentum. Several possibilities have been so far put forward. In the first one (Heller & Shlosman 1994) when the central disc becomes gas dominated it is unstable and breaks into clumps. Via their collisions, these clumps may loose angular momentum and spiral to the center. A second possibility is that the  $x_2$  family does not exist, or that it has a very small extent, in which case the central area is very small. It has, however, been argued that the density distribution in barred galaxies is such as to permit an  $x_2$  family of sizeable extent (e.g. Teuben et al. 1986; Athanassoula 1991, 1992; Athanassoula & Bureau 2000). A similar effect can be achieved in the case of a very high sound speed, in which case the shock loci are very near the center (Englmeier & Gerhard 1997, Patsis & Athanassoula 2000). At somewhat smaller, but still quite high, sound speeds the distance between the main shock loci and the center may be bridged by a spiral, which can also transfer gas to the center (Maciejewski et al. 2002). As a final alternative let me mention nested bars, which can be either gaseous, as initially suggested by Shlosman, Frank & Begelman (1989), or stellar (Erwin, these proceedings). Recent hydrodynamical simulations, however, argue that secondary stellar bars are unlikely to increase the mass inflow rate into the galactic nucleus (Heller & Shlosman 2002, Maciejewski et al. 2002). Further work on this subject is necessary in order to elucidate the properties and the role of secondary bars.

## 8. Bar destruction and regeneration

There are at least two ways by which bars could be destroyed, or, by which their amplitude could be very severely diminished. One can be assimilated to a self-destruction, since the culprit is the central concentration formed by the gas

which is pushed towards the center of the galaxy by the bar itself. In the second method the culprit is a companion or small infalling galaxy.

As mentioned in the previous section, the gas is pushed inwards by the bar. Once it has reached the center, it may create a sufficient central concentration to destroy the bar that drove it there (Friedli & Benz 1993, Berentzen et al. 1998). Indeed, orbital calculations by Hasan & Norman (1990) and by Hasan, Pfenniger & Norman (1993) have shown that a sufficiently strong central concentration can make the  $x_1$  orbits unstable. Norman, Sellwood & Hasan (1996) showed that a massive core, of mass 5% or more of the combined disc and bulge mass, can destroy a bar. Nevertheless, the mass of black holes in disc systems seems to be smaller, by an order of magnitude or more, than what is required by Norman et al. and thus may not be sufficient to destroy bars.

In purely stellar simulations, vertical impacts by a massive companion in the bar area result in a considerable decrease of the bar amplitude, but destruction was so far found only in cases in which the disc thickened so considerably that the galaxy could not be called a disc galaxy anymore (Athanasoula 1996, 1999). On the other hand, destruction seems to be possible for such impacts if a considerable gaseous component is present (Berentzen, Athanasoula, Heller et al., in preparation). If the companion is initially in a near-circular orbit, then it can easily destroy the bar (Athanasoula 1996, 1999), even in simulations with no gaseous component.

Can a disc form a new bar, once its first one has been destroyed? In other words, can more than one bar form consecutively in the same disc? It should be noted that after the demise of the first bar, a disc is inhospitable for a new bar, since it is left with a considerable central concentration and a high velocity dispersion, both factors inhibiting bar growth. Nevertheless, fresh infalling gas may cool the disc and make it again unstable. A first attempt at making a second bar in this way (Sellwood & Moore 1999) proved successful, so further work on this subject should follow.

**Acknowledgments.** I would like to thank A. Bosma, A. Misiriotis, M. Tagger and F. Maset for stimulating discussions and A. Misiriotis and J. C. Lambert for their collaboration on the software calculating the orbital frequencies. Part of this paper was written while I was visiting INAOE. I would like to thank the ECOS-Nord and the ANUIES for financing this trip and INAOE for their kind hospitality.

## References

- Athanasoula, E. 1991, in Dynamics of Disk Galaxies, ed. B. Sundelius (Göteborg: Chalmers Univ. Technology), 149
- Athanasoula, E. 1992, MNRAS, 259, 345
- Athanasoula, E. 1996, in ASP Conf. Ser. Vol. 91, Barred Galaxies, eds. R. Buta, D. Crocker and B. Elmegreen, (San Francisco: ASP), 309
- Athanasoula, E. 1999, in ASP Conf. Ser. Vol. 160, Astrophysical discs, eds. J. A. Sellwood and J. Goodman, (San Francisco: ASP), 160, 351
- Athanasoula, E. 2002, ApJ, 569, L83 (A02)
- Athanasoula, E., Bosma, A., & Papaioannou, S. 1987, A&A, 179, 40

- Athanassoula, E., & Bureau, M. 2000, *ApJ*, 522, 699
- Athanassoula, E., & Misiriotis, A. 2002, *MNRAS*, 330, 35 (AM)
- Athanassoula, E., & Sellwood, J. A. 1986, *MNRAS*, 221, 213
- Berentzen, I., Heller, C. H., Shlosman, I., & Fricke K. J. 1998, *MNRAS*, 300, 49
- Bosma, A. 1999, in ASP conference series 182, *Galaxy Dynamics*, eds. D. R. Merritt, M. Valluri & J. A. Sellwood, 339
- Bosma, A. 2000, in ASP conference Series 197, *From the Early Universe to the Present*, eds. F. Combes, G. A. Mamon & V. Charmandaris, (San Francisco: ASP), 91
- Bottema, R. 1993, *A&A*, 275, 16
- Combes, F., Debbasch, F., Friedli, D., & Pfenniger, D. 1990, *A&A*, 233, 82
- Courteau, S., & Rix, H. W. 1999, *ApJ*, 513, 561
- Debattista, V. P., & Sellwood, J. A. 1998, *ApJ*, 493, L5
- Debattista, V. P., & Sellwood, J. A. 2000, *ApJ*, 543, 704
- Englmaier, P., & Gerhard, O. 1997, *MNRAS*, 287, 57
- Friedli, D., & Benz W. 1993, *A&A*, 268, 65
- Hasan, H., & Norman, C. 1990, *ApJ*, 361, 69
- Hasan, H., Pfenniger, D., & Norman, C. 1993, *ApJ*, 409, 91
- Heller, C. H., & Shlosman, I. 1994, *ApJ*, 424, 84
- Heller, C. H., & Shlosman, I. 2002, *ApJ*, 565, 921
- Hernquist, L., & Weinberg, M. D. 1992, *ApJ*, 400, 80
- Hohl, F. 1971, *ApJ*, 168, 343
- Kawai, A., Fukushige, T., Makino, J., & Taiji, M. 2000, *PASJ*, 52, 659
- Kranz, T., Slyz, A., & Rix, H. W. 2001, *ApJ*, 562, 164
- Little, B., & Carlberg, R. G. 1991, *MNRAS*, 250, 161
- Lynden-Bell, D., & Kalnajs, A. J. 1972, *MNRAS*, 157, 1
- Maciejewski, W., Teuben, P. J., Sparke L. S., & Stone, J. M. 2002, *MNRAS*, 329, 502
- Miller, R. H., Prendergast, K. H., & Quirk, W. J. 1970, *ApJ*161, 903
- Ohta, K. 1996, in ASP conference Series Vol 91, *Barred Galaxies*, eds. R. Buta, D. A. Crocker, B. G. Elmegreen, (San Francisco: ASP), 37
- Patsis, P., & Athanassoula, E. 2000, *A&A*, 358, 45
- Sackett, P. D. 1997, *ApJ*, 483, 103
- Sellwood, J. A. 1999, in ASP conference series 182, *Galaxy Dynamics*, eds. D. R. Merritt, M. Valluri & J. A. Sellwood, (San Francisco: ASP), 351
- Sellwood, J. A., & Moore E. M. 1999, *ApJ*, 510, 125
- Shlosman, I., Frank, J., & Begelman, M. C. 1989, *Nature*, 338, 45
- Teuben, P., Sanders, R. H., Atherton, P. D., & van Albada, G. D. 1986, *MNRAS*, 221, 1
- Tremaine, S., & Weinberg, M. D. 1984, *MNRAS*, 209, 729
- Weinberg, M. D. 1985, *MNRAS*, 213, 451
- Weiner, B. J., Sellwood, J. A., & Williams, T. B. 2001, *ApJ*, 546, 931